

# Diagnostics of Multicomponent Plasma Using EMIC Waves Observed by the Akebono Satellite

メタデータ	言語: eng 出版者: 公開日: 2017-10-05 キーワード (Ja): キーワード (En): 作成者: メールアドレス: 所属:
URL	<a href="http://hdl.handle.net/2297/42264">http://hdl.handle.net/2297/42264</a>

This work is licensed under a Creative Commons Attribution-NonCommercial-ShareAlike 3.0 International License.



---

Abstract

Diagnostics of multicomponent plasma using  
EMIC waves observed by the Akebono satellite

Graduate School of Natural Science and Technology  
Division of Electrical Engineering & Computer Science

Shoya Matsuda

6 January 2015

## Abstract

The Earth's magnetosphere is one of most important topics in terrestrial space physics, and particularly important is the magnetosphere inside a few  $L$  shell, called the Earth's "inner magnetosphere." This inner magnetosphere has a unique structure, particularly a unique spatial particle population. In the present study, we focused on electromagnetic ion cyclotron (EMIC) waves to discuss cold ion composition in the inner magnetosphere. The propagation characteristics of EMIC waves have a close relation to the cold ion composition. Therefore, we can utilize plasma waves as plasma diagnostics tool. We clarified major and minor ion composition and distribution in the inner magnetosphere analyzing characteristic frequencies of typical EMIC waves and ion cyclotron whistler waves observed by the Akebono satellite (e.g., crossover frequency and bi-ion hybrid frequency). For example, it was determined that a certain amount of  $M/Q = 2$  ions (alpha particles or deuterons) exist at  $L$  inside 2.4 in the local dayside and inside 3.0 in the local nightside. Finally, we proposed techniques of plasma wave analyses and specifications of data products for next-generation plasma wave measurements by scientific satellites. Scientific output is expected to increase because of the use of wave power spectra and phase information of observed waveforms.

## 1 General Introduction

The Earth's magnetosphere is one of most important region of terrestrial space physics, especially, the magnetosphere inside a few  $L$  shell is called "the Earth's inner magnetosphere". Energy range of inner magnetospheric particles is from "cold" ( $\sim$  a few eV) to "relativistic" ( $\sim$  a few tens MeV). Excitation and propagation properties of plasma wave strongly depend on energetic and cold plasma particles, respectively.

In this study, we aim to establish a new method of ion composition estimation. A way of estimating cold ion composition is particularly important due to the limitations of particle observation. We focus on the variations of plasma wave properties, particularly those of ion cyclotron mode waves observed by wave instruments onboard scientific satellites. As we mentioned before, the propagation characteristics of ion cyclotron

mode waves have a close relation to the cold ion composition. Therefore, we can utilize plasma waves as plasma diagnostics tool. Our study plays a role in the discovery of inner magnetospheric physics.

## 2 EMIC Waves

Electromagnetic ion cyclotron (EMIC) waves play an important role in inner magnetospheric physics. They are excited by the cyclotron instability of anisotropic energetic ions (with energies of tens of keV) [Cornwall, 1965, Kozyra *et al.*, 1984]. Propagation properties of plasma wave, especially those of an ion cyclotron mode wave, strongly depends on the low-energy ion composition. If there exist two species of major ions,  $H^+$  and  $He^+$ , the dispersion relation of an EMIC wave in cold plasma theory is represented as shown in Figure 1. The coarsely hatched region corresponds to the region of left-handed polarization and the finely hatched region corresponds to the region of right-handed polarization. The relative ion constituents are  $H^+$ :80.0% and  $He^+$ :20.0%.

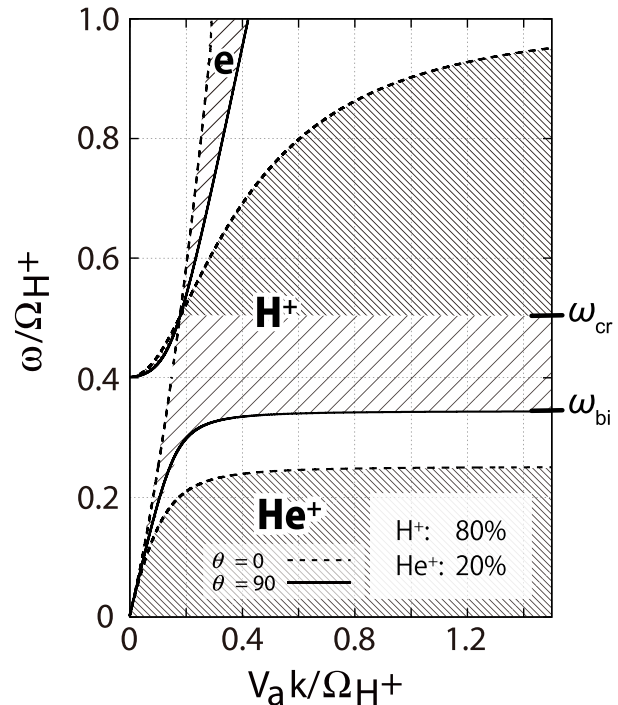


Figure 1. Dispersion curve of an electromagnetic ion cyclotron mode wave. The relative ion constituents are  $H^+$ :80.0% and  $He^+$ :20.0%.

As is well known, EMIC waves in plasmas are usually left-handed polarized. However, in multiple compo-

nent plasma, the dispersion relation of EMIC waves divides into two branches with different characteristics. In Figure 1, the dispersion relation is separated into a  $H^+$  mode ( $\omega/\Omega_{H^+} > 0.35 \mid_{k \rightarrow \infty}$ ) and a  $He^+$  mode ( $\omega/\Omega_{H^+} < 0.25 \mid_{k \rightarrow \infty}$ ). With decreasing frequency of the  $H^+$  mode EMIC wave, the polarization gradually changes from left-handed to linear and finally to right-handed. The frequency at which the EMIC wave becomes linearly polarized is known as the “crossover frequency” ( $\omega_{cr}$ ). The crossover frequency can be theoretically obtained by solving the equation  $n_{\parallel R} = n_{\parallel L}$  as follows:

$$\frac{1}{\Omega_e^2} + \sum_i \frac{A_i}{\left(\frac{m_i}{m_e}\right)^2 \omega_{cr}^2 - \Omega_e^2} = 0. \quad (1)$$

### 3 Akebono Satellite

The Akebono satellite, one of Japan’s science spacecrafts, has successfully observed the auroral region and inner magnetosphere for over 25 years since its launch in February, 1989. Long-term observation data collected by the Akebono satellite cover two cycles of solar activity, providing valuable information on inner magnetospheric physics. The ELF receiver is a subsystem of the VLF instrument onboard Akebono. The ELF receiver operates in two modes: ELF-NARROW mode, which measures waveforms below 50 Hz for one component of the electric field and three components of the magnetic field, and ELF-WIDE mode, which measures waveforms below 100 Hz for one component of the electric and magnetic fields [Kimura *et al.*, 1990]. Ion cyclotron wave observations were reported near the geomagnetic equator by the ELF receiver [Kasahara *et al.*, 1992].

### 4 EMIC waves suggesting minor ion existence

Figure 2 shows electric field wave spectrum below 60 Hz measured by the ELF receiver from 06:11:10 to 06:18:50 UT on April 15, 1989. Thick dashed line in the spectrogram indicates  $\Omega_{He^+}$ , where  $\Omega_i$  denotes the local cyclotron frequency of ion species “ $i$ ”. Thin dashed line in the spectrogram indicates “ $0.5\Omega_{H^+}$ ”.

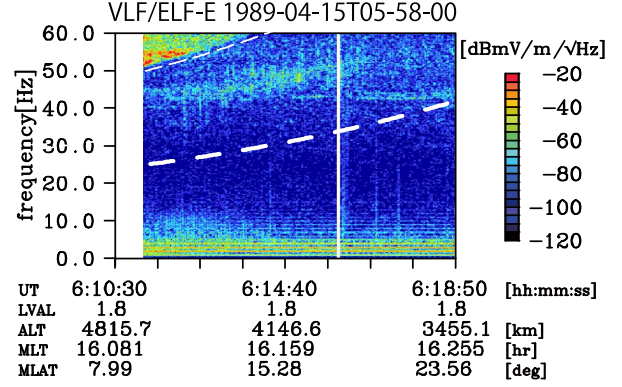


Figure 2. Electric field wave spectrogram of ELF emissions observed on April 15, 1989.

As shown in the figure, a band of emission was commonly observed around 30–60 Hz, and the emission exhibited a sudden decrease in intensity at  $0.5\Omega_{H^+}$  along the trajectory of Akebono across the magnetic equator within  $\pm 15$  degrees of magnetic latitude. According to our analysis, a crossover frequency exists above the characteristic lower cutoff, and these EMIC waves have left-handed polarization in the higher-frequency parts, while the polarization gradually changes to linear and finally to right-handed in the lower-frequency parts of the waves. It was demonstrated that these events follow the linear theory of EMIC waves with multiple ion constituents. We have also noted that another band of EMIC waves were simultaneously observed below  $0.5\Omega_{H^+}$  on April 15 and on April 25, 1989.

Comparing the variations in the Dst index with the time when EMIC waves were observed with their characteristic lower cutoff, the waves were repeatedly observed within half a day after sudden decreases in Dst. Although stormy conditions existed, such as an increase in the Dst index to  $-130$  nT, the characteristic lower cutoffs of each event were stable at just above  $0.5\Omega_{H^+}$ . We studied the dispersion relation of EMIC waves under the condition of multiple ion species and demonstrated that the lower cutoff of the EMIC wave can be explained when the inner magnetosphere consists of a few percent alpha particles ( $He^{++}$ ) or deuterons ( $D^+$ ).

We can clearly explain the lower cutoff of the EMIC wave just above  $0.5\Omega_{H^+}$ . When we assume three types of ions  $H^+$ ,  $He^+$ , and  $He^{++}$  in the plasma, the dispersion relation of the EMIC wave is shown in Figure 3. The relative ion constituents are  $H^+$ :78.0%,  $He^+$ :20.0%, and  $He^{++}$ :2.0%. We also superposed a

dispersion curve, represented by a chain line, which corresponds to the perpendicular branch of an EMIC wave with constituents  $H^+$ :88.0%,  $He^+$ :10.0%, and  $He^{++}$ :2.0%.

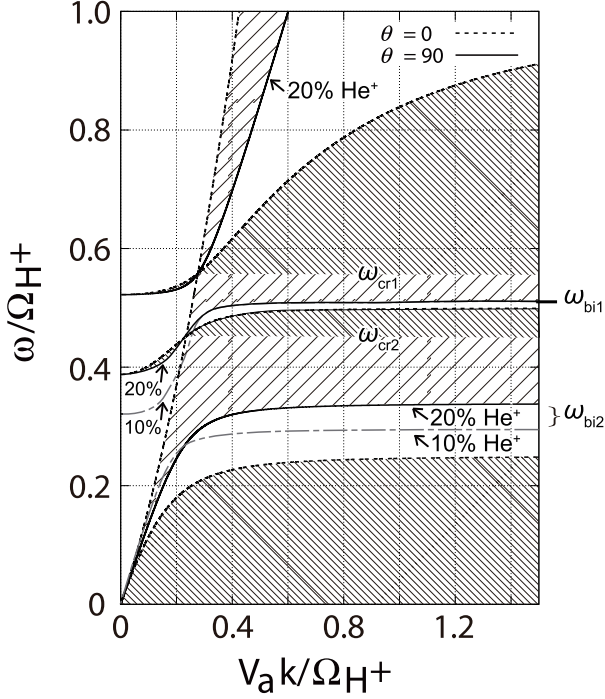


Figure 3. Dispersion curve of an electromagnetic ion cyclotron mode wave. The relative ion constituents are  $H^+$ :78.0%,  $He^+$ :20.0%, and  $He^{++}$ :2.0%. We also superposed a dispersion curve represented by a chain line, which corresponds to the perpendicular branch of an EMIC wave with constituents  $H^+$ :88.0%,  $He^+$ :10.0%, and  $He^{++}$ :2.0%.

As shown in the figure, a new stop band near  $\Omega_{He^{++}} = 0.5\Omega_{H^+}$  appears. The dispersion of the  $H^+$  branch is separated into two branches: a  $H^+$  branch and a  $He^{++}$  branch. The upper cutoff of the  $He^{++}$  branch approaches  $\Omega_{He^{++}}$ . On the other hand, the lower cutoff of the  $H^+$  branch becomes slightly higher than  $\Omega_{He^{++}}$ .  $\omega_{bi1}$  is basically unrelated to the  $He^+$  concentration. In fact, we confirmed that the variation in  $\omega_{bi1}$  is within  $0.01\Omega_{H^+}$ , even though the  $He^{++}$  concentration varies by several percent. In such conditions, another band of the EMIC wave observed on April 15 below  $0.5\Omega_{H^+}$  can also be explained by the fact that they are EMIC waves of the  $He^{++}$  or  $D^+$  branch caused by the existence of such minor ions. We suggest that the EMIC waves that have a lower cutoff just above  $0.5\Omega_{H^+}$  provide evidence for the existence of minor ions with cyclotron frequencies of  $0.5\Omega_{H^+}$ .

## 5 Ion Cyclotron Whistler Waves Observed by the ELF Receiver

It is well known that lightning whistler waves are caused by lightning discharge; these waves propagate along geomagnetic field lines as R-mode plasma waves of less than several tens kHz. Ion cyclotron whistler waves, which are EMIC mode waves, have a close relation to lightning whistlers.

Figure 4 represents a schematic diagram of the propagation mechanism of an ion cyclotron whistler wave. We assumed that a lightning whistler in the R-mode branch is generated in the ionosphere and propagates along the geomagnetic field line toward the opposite hemisphere. The bottom six panels show the time variation of the spectrum pattern when we assume that an R-mode lightning whistler wave is completely converted into an L-mode ion cyclotron wave at the crossover frequency as the wave propagates along the geomagnetic field line. Blue solid lines denote unconverted R-mode lightning whistlers. The wave energy of the frequency range, which is represented by the light-blue dashed lines, was already converted into an L-mode ion cyclotron mode wave.

A converted L-mode ion cyclotron whistler changes its spectrum pattern as it propagates along the geomagnetic field line because its group velocity decreases when the wave frequency approaches the local ion cyclotron frequency. As the wave approaches the geomagnetic equator, the intensity of the background magnetic field  $|B|$  becomes relatively weak. Consequently, local ion cyclotron ( $\Omega_i$ ) and crossover frequencies ( $\omega_{cr_i}$ ) become relatively lower than those in the high-latitude region. In other words, a lightning whistler waves are converted into ion cyclotron whistler waves from higher to lower frequencies. As shown in the dispersion relation (Figure 1), the upper limit frequency of each ion band EMIC approaches each ion cyclotron frequency and cannot propagate further when the wave frequency becomes larger than the local cyclotron frequency. Hence, the asymptotic frequency of an ion cyclotron whistler denotes the frequency just below that of the local ion cyclotron. This process explains formation of the characteristic spectrum delay (from “A” to “F”).

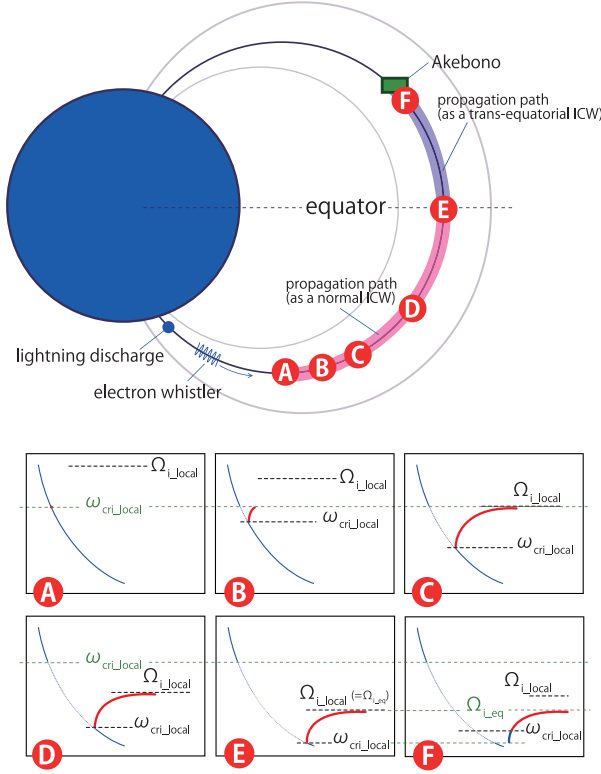


Figure 4. Schematic diagram of the mechanism of ion cyclotron whistler wave generation. The bottom six panels show the time variation of the spectrum pattern.

### 5.1 Case studies of $M/Q = 2$ ion cyclotron whistlers

The top panel of Figure 5 shows the electric field wave spectrum below 80 Hz measured by the ELF receiver from 04:57:47 to 04:57:51 UT on May 15, 1989. The bottom panel of Figure 5 shows a schematic diagram of the wave. Thick dashed lines and chain lines in the panels indicate  $\Omega_{He^+_{local}}$  and  $\Omega_{O^+_{local}}$ , respectively, where  $\Omega_{i_{local}}$  denotes the local cyclotron frequency of ion species “ $i$ ” along the trajectory. Thin dashed lines indicate “ $0.5 \Omega_{H^+_{local}}$ ”.

This event was observed when Akebono was orbiting from the southern to the northern hemisphere in the altitude region around 4200 km on the day side. As shown in Figure 5, a lightning electron whistler (shown as (O) in the bottom panel of Figure 5) was observed around 10–56 Hz from 04:57:48 to 04:57:49 UT. Furthermore, an  $M/Q = 2$  ion cyclotron whistler (shown as (A) in the bottom panel of Figure 5) was simultaneously observed around 46–56 Hz. This  $M/Q = 2$  ion cyclotron whistler had an asymptotic frequency approaching  $0.5 \Omega_{H^+_{local}}$ . In addition,

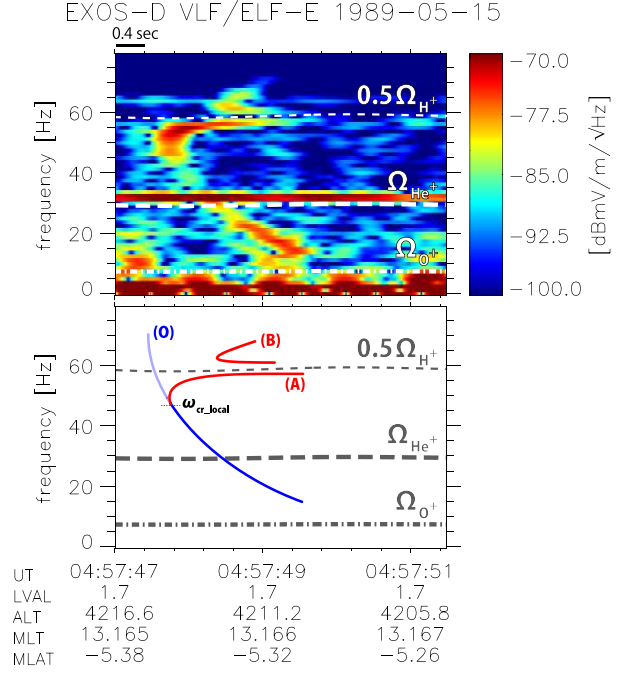


Figure 5. (top) Electric field spectrogram of the  $M/Q = 2$  ion and  $H^+$  mode cyclotron whistlers observed on May 15, 1989. (bottom) Schematic diagram of the wave.

a  $H^+$  cyclotron whistler (shown as (B) in the bottom panel of Figure 5) was simultaneously observed above  $0.5 \Omega_{H^+_{local}}$ .

We examine ion concentrations during the event. As shown in equation (1) in the previous section, the crossover frequencies of ion cyclotron mode waves are closely related to the ion concentration ratio in plasma. As a general rule, if there are  $p(\geq 2)$  types of ions, crossover frequencies appear on  $(p - 1)$  ion branches. For example, when we consider three types of ions ( $H^+$ ,  $M/Q = 2$  ion, and  $He^+$ ) to explain the generation of  $M/Q = 2$  ion cyclotron whistlers, two crossover frequencies ( $\omega_{cr1}$  and  $\omega_{cr2}$ ) appear on the  $H^+$  branch and the  $M/Q = 2$  ion branch, respectively. Then we can establish two equations by substituting  $\omega_{cr1}$  and  $\omega_{cr2}$  in equation (1). In addition, the total ion concentration ratio  $\sum_i A_i$  equals 1, i.e.,  $A_{H^+} + A_{M/Q=2} + A_{He^+} = 1$ . The ion mass ( $m_i$ ), electron mass ( $m_e$ ), and electron cyclotron frequency ( $\Omega_e$ ) in equation (1) are known parameters in the equation. If we can determine two crossover frequencies ( $\omega_{cr1}$  and  $\omega_{cr2}$ ) by observation, we can completely estimate the unique concentration of ions ( $A_{H^+}$ ,  $A_{M/Q=2}$ ,  $A_{He^+}$ ) by solving the simultaneous equations.

We estimated the ion concentration from the crossover frequency of an  $M/Q = 2$  ion cyclotron whistler ob-



served at 04:57:45 UT on May 15, 1989 (shown as (A) in the bottom panel of Figure 5). The existence of such crossover frequency suggests that some “ $M/Q = 2$  ions” and “heavier ions than  $M/Q = 2$ ” were present along the trajectory. Estimation was based on the following assumptions:

- There were three types of ions ( $H^+$ ,  $D^+$ ,  $He^+$ ).
- The  $He^+$  concentration was in the range 10–20% (the typical range for  $He^+$  concentration in the plasmasphere [Lemaire *et al.*, 1998]).

Figure 6 shows the relationship between the  $He^+$  concentration (horizontal axis) and the  $M/Q = 2$  ion concentration (vertical axis) for a crossover frequency of  $M/Q = 2$  ion band of 45.6 Hz (red line). Furthermore, we show the error range lying between the gray dotted lines at 45.0 Hz and 46.3 Hz, which is derived from the errors in crossover frequency determination caused by the resolution of fast Fourier transform analysis. For example, the concentration of  $M/Q = 2$  ions is estimated to be 9.41–12.6% when we assume a  $He^+$  level of 20.0%. Note that the concentration of  $He^+$  is generally suggested to be 10–20%, and  $He^+$  of 20% is at the upper bound of the typical ion concentration. This suggests that the actual concentration of  $M/Q = 2$  ions is lower than 12.6%. It should also be noted that the red line in Figure 6 crosses the horizontal axis at  $He^+$  concentration of 9.95–10.95%; this suggests that a value of more than 9.95% of  $He^+$  along the trajectory is a requirement for consistency with the observation of  $M/Q = 2$  ion cyclotron whistlers.

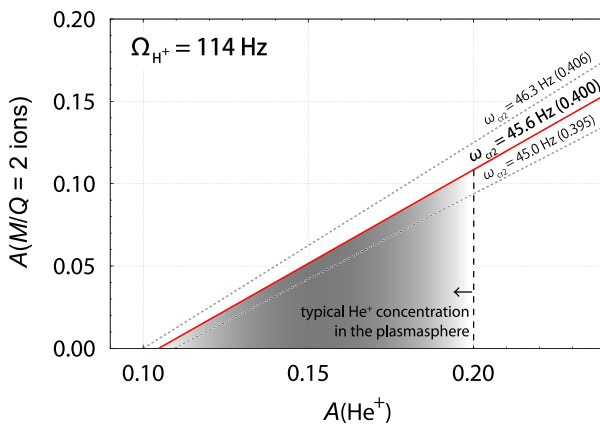


Figure 6. Relationship between the  $He^+$  concentration (horizontal axis) and the  $M/Q = 2$  ion concentration (vertical axis) for a crossover frequency of the  $M/Q = 2$  ion band of 45.6 Hz (red line).

## 5.2 Statistical study of ion cyclotron whistlers

We analyzed the waveform data observed by the ELF receiver in both ELF-WIDE and ELF-NARROW modes during a six-year, seven-month period from March 1989 to September 1995. We detected 845  $H^+$  band ion cyclotron whistlers, 933  $M/Q = 2$  ion band ion cyclotron whistlers, and 1888  $He^+$  band ion cyclotron whistlers by visual inspection during the study period. Spatial distributions of  $H^+$  band (a and d),  $M/Q = 2$  ion band (b and e), and  $He^+$  band (c and f) ion cyclotron whistler waves observed by the Akebono satellite. The top three panels (a, b, and c) and the bottom three panels (d, e, and f) represent local dayside (06–18 MLT) and local nightside (18–06 MLT) observation, respectively.

A comparison of the spatial occurrence distributions of local day- and nightside events revealed some important features, as are shown in Figure 7. The region in which  $H^+$  band ion cyclotron whistler waves were not observed near the equator was wider in the local nightside than that in the local dayside (Figures 7a and 7d). For  $M/Q = 2$  ion cyclotron whistler waves (Figures 7b and 7e), occurrence frequency was higher near the equatorial region in the local nightside than that in the local dayside. Furthermore, the region wherein  $M/Q = 2$  ion cyclotron whistlers were observed was distributed in a wider  $L$  shell range in the local nightside than that in the local dayside. This fact suggests that the spatial occurrence distributions of these two band events are nearly exclusive. For local dayside,  $M/Q = 2$  ion cyclotron whistlers were observed around  $L$  from 1.6 to 2.4. Conversely, for local nightside, they were observed around  $L$  inside 2.3.

We estimated the ion combination by considering the minimum conditions necessary for ion cyclotron whistler generation. We assumed that certain amounts of  $H^+$  and  $He^+$  can exist anywhere in the plasmasphere [Lemaire *et al.*, 1998]. In Figure 8, we show estimated  $M/Q = 2$  ion distributions in schematic diagrams. Left and right panels show that in local day- and nightside, respectively. The region where  $M/Q = 2$  ion cyclotron whistlers were observed (Figures 7b and 7e) undoubtedly indicates existence of a certain amount of  $M/Q = 2$  ions (blue shaded regions in Figure 8). The question is whether  $M/Q = 2$  ions exist or not in the other regions.

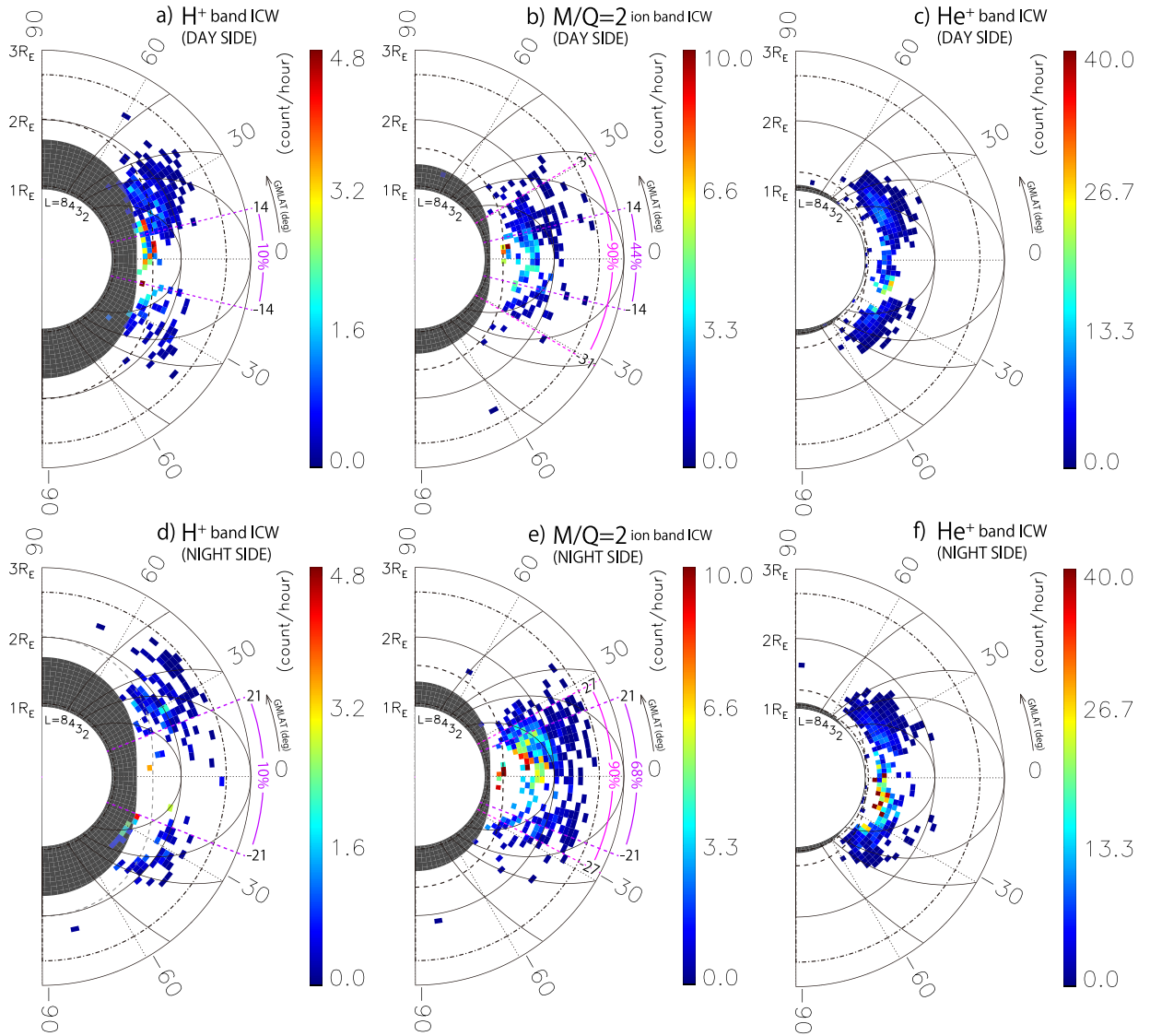


Figure 7. Spatial distributions of  $H^+$  band (a and d),  $M/Q = 2$  ion band (b and e), and  $He^+$  band (c and f) ion cyclotron whistler waves observed by the Akebono satellite. The top three panels (a, b, and c) and the bottom three panels (d, e, and f) represent local dayside (06–18 MLT) and local nightside (18–06 MLT) observation, respectively.

$H^+$  band ion cyclotron whistlers were frequently observed except in the equatorial region (Figures 7a or 7d). As previously mentioned, almost no  $M/Q = 2$  ion band ion cyclotron whistler was observed at this region (Figures 7b or 7e), nor was an  $He^+$  band ion cyclotron whistler (Figures 7c or 7f). In the existence of a certain amount of  $M/Q = 2$  ions,  $M/Q = 2$  ion band ion cyclotron whistlers should be observed. However, in fact, they were not observed. Hence, almost no  $M/Q = 2$  ions near this region affect wave generation and propagation (gray shaded regions in Figure 8).

$He^+$  band ion cyclotron whistlers were frequently observed at an altitude region below approximately

$1.7R_E$  (Figures 7c or 7f), however, show the occurrence frequency of  $M/Q = 2$  ion band ion cyclotron whistlers to be quite low (Figures 7b or 7e). In this situation, we cannot determine whether  $M/Q = 2$  ions exist in this region because when an  $He^+$  band ion cyclotron whistler is generated along a geomagnetic field line, an  $M/Q = 2$  ion cyclotron whistler rarely generates along the same geomagnetic field line (pink shaded regions in Figure 8). This is an ambiguous point in our estimation. Even so, the present result provided new findings of minor ion distribution in the plasmasphere.

In summary, it was determined that a certain amount of  $M/Q = 2$  ions exist at  $L$  inside 2.4 in the local dayside



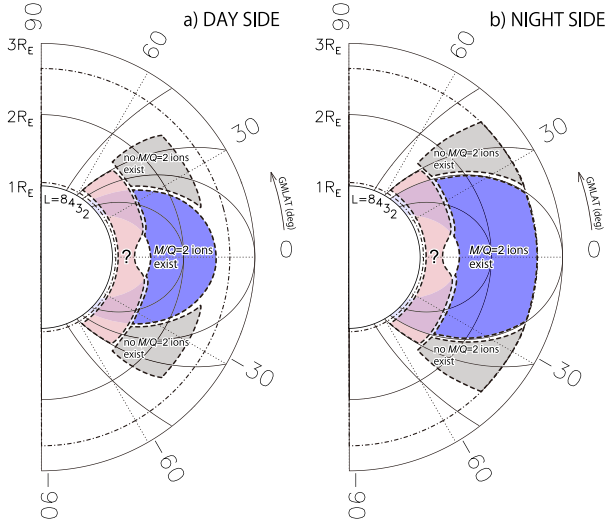


Figure 8. Schematic diagrams of estimated  $M/Q = 2$  ion distributions. Left and right panels show that in local day- and nightside, respectively. Blue shaded regions indicate the regions where  $M/Q = 2$  ions exist. Gray shaded regions indicate the regions where no  $M/Q = 2$  ions exist. Pink shaded regions indicate the regions where we cannot determine whether  $M/Q = 2$  ions exist.

and inside 3.0 in the local nightside. The generation conditions of  $H^+$  band ion cyclotron whistler waves are closely related to those of  $M/Q = 2$  ion band ion cyclotron whistler waves. Such  $M/Q = 2$  ions appeared to be  $D^+$  of ionospheric origin because the relative occurrence frequency of observed  $M/Q = 2$  ion cyclotron whistlers was higher near the low- $L$  shell region than that near the high- $L$  shell region.

## 6 Proposal for Future Satellite Mission

We propose techniques of plasma wave analyses and specifications of data products for next-generation plasma wave measurements by scientific satellites. Scientific output is expected to increase because of the use of wave power spectra and phase information of observed waveforms.

The traditional data product is shown in Table 1 (MODE A). One component of electric and magnetic field wave spectra are observed by MODE A. One spectrum is observed every 0.25 seconds. Frequency components of observed wave spectra are explained by 92 logarithmically spaced frequency bins.

Table 1. Data products and their specification in MODE A.

Data	Specification
Power spectrum (E)	4 Hz x 8 bit x 92 point x 1 ch
Power spectrum (B)	4 Hz x 8 bit x 92 point x 1 ch
Total amount	5.88 kbps

MODE B is one of our proposed data products. It observes wave power spectra of electric and magnetic fields, phase difference, and axial ratio between any two components of the observed magnetic field (Table 2). Before phase difference and axial ratio calculation, coordinate transformation is applied to the observed magnetic field waveform. Instead of increasing the number of types of data product, the frequency resolution of each data product is reduced.

Table 2. Data products and their specification in MODE B.

Data	Specification
Power spectrum (E)	4 Hz x 8 bit x 46 point x 1 ch
Power spectrum (B)	4 Hz x 8 bit x 46 point x 1 ch
Phase difference (B)	4 Hz x 8 bit x 46 point x 1 comp
Axial ratio (B)	4 Hz x 8 bit x 46 point x 1 comp
Total amount	5.88 kbps

MODE C is our second proposed data product. It observes one component of the electric field wave spectrum and the spectral matrix of the observed magnetic field wave (Table 3). The spectral matrix contains the full phase information of the observed field wave. In addition, we can apply coordinate transformation using an observed spectral matrix after the raw data is transmitted to the ground. Therefore, onboard coordinate transformation is not required in this observation mode. Hence, total calculation cost will be reduced by operating in this mode. This mode provides various physical data; however, frequency resolution should be decreased to satisfy the data capacity of the telemetry.

Table 3. Data products and their specification in MODE C.

Data	Specification
Power spectrum (E)	4 Hz x 8 bit x 46 point x 1 ch
Spectral matrix (B)	4 Hz x 8 bit x 23 point x 6 comp
Total amount	5.88 kbps

We evaluate the computation cost required to operate each mode. Figure 9 represents the comparison of

computation time required to operate each mode on the computer. Computation time represented in the figure is normalized using that of the traditional mode (labeled “as usual” in Figure 9). Traditional mode independently calculates the STFT of each component and then applies averaging. MODE A outputs the same data types as traditional mode; however, computation time is reduced by approximately half due to the our proposed FFT technique. MODE B contains computations of phase difference and axial ratio, which occupy approximately 5% of the entire computation time. However, appropriate coordinate transformation is necessary to derive phase difference and axial ratio in any plane. Therefore, additional time is required to read satellite position data and to operate coordinate transformation of observed data, which becomes a bottleneck. The computation time of MODE C is increased by 10% over MODE A. As mentioned before, additional coordinate transformation is not necessary when we operate MODE C. Hence, the total computation time of MODE C seems to be shorter than that of MODE B. However, resolution of output is sacrificed when we operate MODE C. Considering whether the selected mode satisfies the requirements of observation is necessary.

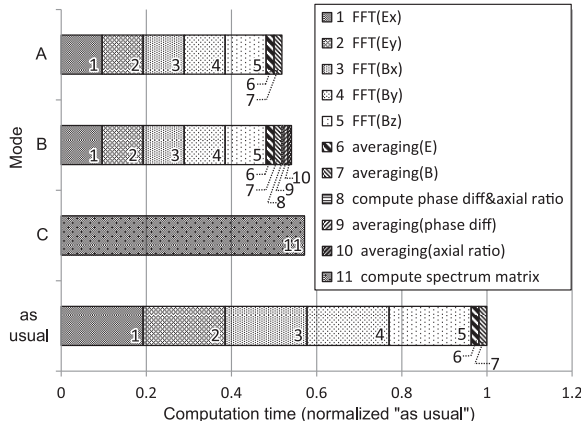


Figure 9. Comparison at computation time of each mode

## 7 Summary

In the present study, we have focused on the EMIC wave and have investigated a new method of cold ion composition estimation. We have introduced typical EMIC waves observed by the Akebono satellite. These EMIC waves were observed from a few Hz to a few tens Hz (below local proton cyclotron frequency  $\Omega_{H^+}$ ) during duration of typical EMIC wave ( $\sim$  a few tens

minutes). It has been found that EMIC waves which had characteristic cutoff frequency just above half of proton cyclotron frequency ( $0.5\Omega_{H^+}$ ) were frequently observed at an altitude region around a few thousand km by the Akebono satellite. These events have suggested that the existence of  $M/Q = 2$  ion at the local point and the propagation path of the wave. Our statistical study suggested that upper limit of estimated  $M/Q = 2$  ion composition is 4.6%.

We have discussed ion cyclotron whistlers observed by the Akebono satellite. We have surveyed frequency-time spectra of observed electric and magnetic field wave, and found that 3775 ion cyclotron whistler waves were observed. Other than major ion ( $H^+$ ,  $He^+$ , and  $O^+$ ) band ion cyclotron whistlers, a lot of minor ion ( $M/Q = 2$  ion and  $M/Q = 8$  ion) band ion cyclotron whistlers were observed by the receiver. This has been the clear evidence which suggests existence of such minor ions in the inner magnetosphere. We have statistically studied observed ion cyclotron whistler waves, and clarify spatial distributions of their occurrence frequencies. It has been found that  $H^+$  ion cyclotron whistler waves hardly observed around the equatorial region. Additionally, diurnal dependence of  $M/Q = 2$  ion distribution has found. It has been found that  $M/Q = 2$  ions which can affect wave propagation exists inside  $L \sim 2.5$  on local day-side (06–18 MLT) and inside  $L \sim 3.0$  on local night-side (18–06 MLT). Hence, it has been suggested that existence of density enhancement process of  $M/Q = 2$  ion on local night-side inner magnetosphere.

We have proposed new techniques and observation modes for a new-generation onboard software wave receiver. We have proposed two novel data products and compared advantages and disadvantages of each data product. To reduce computation time, we have proposed new techniques of method of transforming observed data from time domain to frequency domain, trigonometric function calculation, phase difference calculation, and averaging. We have evaluated computation time and accuracy of proposed techniques. Finally, we have evaluated total computation time of proposed observation modes. We have confirmed that the computation time of each mode satisfy limitation of onboard processing unit.

---

## References

- Cornwall, J. M. (1965), Cyclotron instabilities and electromagnetic emission in the ultra low frequency and very low frequency ranges, *J. Geophys. Res.*, 70(1), 61–69, doi:10.1029/JZ070i001p00061.
- Gurnett, D. A., S. D. Shawhan, N. M. Brice, and R. L. Smith (1965), Ion cyclotron whistlers, *J. Geophys. Res.*, 70(7), 1665–1688, doi:10.1029/JZ070i007p01665.
- Kasahara, Y., A. Sawada, M. Yamamoto, I. Kimura, S. Kokubun, and K. Hayashi (1992), Ion cyclotron emissions observed by the satellite Akebono in the vicinity of the magnetic equator, *Radio Sci.*, 27(2), 347–362.
- Kimura, I., K. Hashimoto, I. Nagano, T. Okada, M. Yamamoto, T. Yoshino, H. Matsumoto, M. Ejiri, and K. Hayashi (1990), VLF Observations by the Akebono (EXOS-D) satellite, *J. Geomag. Geoelectr.*, 42, 459–478.
- Kozyra, J. U., T. E. Cravens, A. F. Nagy, E. G. Fonthelm, and R. S. B. Ong (1984), Effects of energetic heavy ions on electromagnetic ion cyclotron wave generation in the plasmopause region, *J. Geophys. Res.*, 89(A4), 2217–2233, doi:10.1029/JA089iA04p02217.
- Lemaire, J. F., K. I. Gringauz, D. L. Carpenter, and V. Bassolo (1998), *The Earth's Plasmasphere*, Cambridge Atmospheric and Space Science Series, Cambridge University Press.



## 学位論文審査報告書（甲）

1. 学位論文題目（外国語の場合は和訳を付けること。）

Diagnostics of multicomponent plasma using EMIC waves observed by the Akebono satellite (和訳) あけぼの衛星で観測された EMIC 波動解析に基づくプラズマ診断

2. 論文提出者 (1) 所 属 電子情報科学 専攻

(2) 氏 名 松田 昇也

3. 審査結果の要旨（600～650 字）

平成 27 年 2 月 4 日に第 1 回学位論文審査委員会を開催した後、口頭発表を行った。その直後に、第 2 回審査委員会を開いて慎重審議を行った結果、以下の通り判定した。なお、口頭発表における質疑を最終試験に代えるものとした。

地球周辺の宇宙プラズマ空間は、太陽フレアや電離層擾乱など、様々な要因で日々劇的に変動するが、特に内部磁気圏と呼ばれる領域は、プラズマ粒子と波動が相互作用を起こし、人工衛星や宇宙飛行士に多大な影響を及ぼす。イオンサイクロトロン波 (EMIC) は、同領域の代表的なプラズマ波動であるが、本研究ではあけぼの衛星による電磁波観測データから、質量対電荷比 ( $M/Q$ ) が 2 のイオンに起因する EMIC の存在を示し、磁気圏内でマイナーとされていた  $M/Q=2$  イオンが、磁気赤道を中心に広範囲に分布することを実証した。また長期観測データを用いた統計解析から、ローカルタイムや太陽活動度によって、内部磁気圏プラズマ中で同イオンが占める比率が変動することも示した。さらに本研究では、同成果を踏まえて将来の科学衛星で波動観測器によるプラズマ環境計測に要求される性能を達成するための機上処理法も提案している。これらの成果は、内部磁気圏を観測・理解するうえで非常に重要であり、今後の内部磁気圏物理の研究に大きく貢献するものである。以上より、本論文は博士（工学）に値すると判定した。

4. 審査結果 (1) 判 定 (いずれかに○印) 合 格 ・ 不合格

(2) 授与学位 博 士 ( 工 学 )